Optical response of layers of embedded semiconductor quantum dots

C. M. J. Wijers and Jiun-Haw Chu
Department of Electronic Engineering and Institute of Electronics, National Chiao Tung University, 1001 Ta Hsueh Road, Hsinchu 300, Taiwan

J. L. Liu
Department of Applied Mathematics, National University of Kaohsiung, Kaohsiung 811, Taiwan

O. Voskoboynikov
Institute of Electronics and Department of Electronic Engineering, National Chiao Tung University, 1001 Ta Hsueh Road, Hsinchu 300, Taiwan

(Received 12 April 2006; published 19 July 2006)

The influence of the surrounding semiconducting matrix upon the polarizability of embedded nanoobjects (quantum dots) has been investigated. The previously proposed hybrid model has been extended to accommodate the influence of embedding. It turns out that excess discrete dipoles having an excess polarizability against a uniform background identical to the dielectric host material build the basis for a modified discrete dipole model, suited to describe the optical response of this system. The individual dipoles are described by means of dielectric embedded oblate ellipsoids as to their static response. An efficient description of the electrostatics of these ellipsoids has been given in terms of explicit functions using cylindrical coordinates and compatible with similar derivations for spherical dielectric objects. The dynamic contribution, responsible for frequency dependence is determined quantum mechanically and added to the embedded bare polarizability. The result of the model for the particular InAs quantum dot GaAs host combination investigated is a slightly decreased internal reflectance as compared to vacuum and an overall strong increment of the absorbance, the structure in the reflectance and of the ellipsometric angles.

DOI: 10.1103/PhysRevB.74.035323 PACS number(s): 73.21.−b, 75.20.Ck, 75.75.+a

I. INTRODUCTION

To make materials from at least two other materials (elementary or compound) by changing the dimensions and geometry of their interface is the essence of metamaterials research. Modern metamaterials research concentrates upon dimensions in the nanometer range. Especially the construction of metamaterials based upon III-V semiconductor nanoobjects (nanosized quantum dots, nanorings, etc.) is a promising field of research, particularly for its high potential to develop optical applications. The present quest for negative refractive index materials[1–3] is a good example of such research opening a completely unorthodox field of optics. Negative refractive index metamaterials have been made in the frequency range up to THz,[4] but the building blocks of these metamaterials were mm sized. Smaller building blocks will be required to move the desired material characteristics to higher frequencies and semiconductor nano-objects are ideal candidates. This kind of research will need appropriate model descriptions to guide it. In the traditional use of nano-object based metamaterials for lasing applications the modelling focuses upon photoluminescence and spontaneous emission, but such modelling is not really adequate for metamaterials such as negative refractive index materials. Then a proper description of the basic linear optical properties of these materials is a first necessity. In two previous papers we have addressed already some fundamental issues concerning this problem, but those papers treated only isolated nano-objects.[5,6] The next step to make this model of real use is to put these nano-objects in a suitable host material. In other words, we want to know what happens with the (linear) optical properties of the nano-objects upon embedding, and this is the question this paper wants to address for composite nano-object metamaterials.

We consider a metamaterial build from nano-objects of characteristic size a. For such a system we assume

$$\lambda \gg a_L > a,$$

where λ is the wavelength of the electromagnetic wave and a_L an average distance between the nano-objects in the metamaterial. We will start our treatment by explaining the difference between bare and dressed polarizabilities for the case of embedded nano-objects and consider the commonly known problem of the dielectric sphere in an external field. This sphere, as we will show, can be replaced by a discrete excess dipole and a corresponding excess polarizability. As a result an ensemble of these nano-objects can effectively be treated by means of modified discrete dipole theory, where frequency dependence enters the modelling through quantum mechanics, as treated before by the authors of this paper.[6] The response of an embedded dielectric ellipsoidal nano-object is subsequently added to the description in order to model as closely as possible realistic semiconductor quantum dots. The resulting hybrid model will be used to treat the change in optical properties of semiconducting nanosized objects (InAs quantum dots) upon embedding in a foreign semiconducting host material (GaAs). Hybrid means for this model that we combine the discrete nonlocal description for the excess response of the dots with a local continuum description for a uniform background, extending over the host material, but also over the dots. Temperature dependence

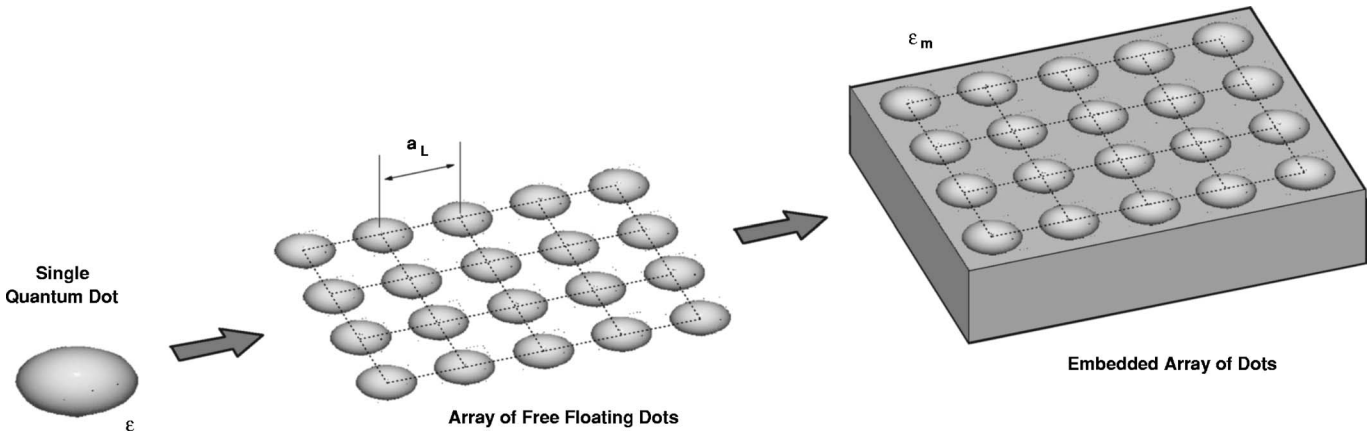

FIG. 1. Conceptual picture of the building of a metamaterial from semiconductor nano-objects (embedded ellipsoidal quantum dots).

will not be taken into account, which means for this paper that the calculations will relate to the $T=0$ K situation. Also aspects of nonlocal quantum mechanical interactions, since those involve typical surface effects which are ignored already implicitly in the envelope function approximation, will be left out from consideration, although we have investigated those in detail in the past for different systems.[7]

II. THEORY

In this section we will derive the hybrid model we will use to describe the optical response of metamaterials composed of nano-objects like quantum dots, embedded in a dielectric host material (see Fig. 1). The nano-objects will be assumed in this paper to have a dielectric constant ϵ different from the dielectric constant ϵ_m of the host material.

In order to keep the paper more transparent we will use during the derivation of the model itself the more familiar and simpler dielectric spheres, to represent the nano-objects. The use of that representation allows for a stronger focus upon the main issue: the consequences of embedding upon the optical properties of an ensemble of nano-objects, in this case a square lattice of quantum dots. For the actual calculations, as told before, flat oblate ellipsoidal dielectric nano-objects will be used. A derivation of the required electromagnetic properties of these ellipsoidal bodies is given in the Appendix. This derivation is such that it can be joined smoothly with the spherical body treatment by replacing a minimum of characterizing parameters.

A. Bare and dressed polarizabilities of semiconductor nano-objects

Quantum dots are generally classified as artificial atoms. Therefore their optical response should also be described in an atomiclike fashion, e.g., by means of polarizabilities. Optics in combination with quantum dot structures relies either upon expressions for optical absorption[8] or upon oscillator strengths,[9,10] being the squared modulus of the optical transition matrix element.[11] The proper approach should be to use the Kramers-Heisenberg expressions, but it is not straightforward to apply those to the case of a dot, described by means of envelope functions.[6] This holds even more when we have to model embedded nano-objects by means of a hybrid description. Then it becomes necessary to distinguish adequately between bare and dressed polarizabilities, although we have used those already implicitly in our previous papers.[5,6] From Ref. 6 we summarize the important definitions. The *dressed* polarizability α_D is defined by

$$\mathbf{p} = \overleftrightarrow{\alpha}_D \mathbf{E}_L, \tag{1}$$

where $\mathbf{E}_L$ is the classical local field, which equals the external field $\mathbf{E}_X$ for the case of a single nano-object. This polarizability is the polarizability which follows directly from experimental observations, since the external field is measurable. The *bare* polarizability α_B is defined with respect to the applied electric field $\mathbf{E}_A$ by

$$\mathbf{p} = \overleftrightarrow{\alpha}_B \mathbf{E}_A,$$

$$\mathbf{E}_A = \mathbf{E}_L + \overleftrightarrow{\mathbf{t}}\mathbf{p}, \tag{2}$$

where $\mathbf{t}$ is the full electromagnetic selfinteraction tensor for the nano-object, to be called further intracellular transfer tensor. It is easily verified that for the case of a dielectric sphere or ellipsoid, the applied field equals statically the internal field. For that case it is also the average electric field. The bare polarizability α_B is not measurable and the only way to obtain it independently is by means of theory. Further we repeat from Ref. 6 the elementary relationship between the two kinds of polarizability:

$$\overleftrightarrow{\alpha}_D^{-1} = \overleftrightarrow{\alpha}_B^{-1} - \overleftrightarrow{\mathbf{t}}. \tag{3}$$

The distinction between bare and dressed polarizabilities, although not always under these labels, is old and goes back to the discussion about the validity of the Sellmeier and Lorentz-Lorenz, Clausius-Mossotti descriptions.[12,13] The distinction however is still relevant and here necessary even to understand properly the physics behind the hybrid method.

The key reason why for hybrid models the distinction between bare and dressed polarizabilities needs to be emphasized concerns the fundamental issue to which static polarizability the dynamical contribution $\Delta\alpha$, as derived before in[6]

$$\Delta\alpha(\omega) = \frac{3}{4}\frac{e^2}{\hbar} r_{eh}^2 (\hat{\mathbf{x}}\hat{\mathbf{x}}^T + \hat{\mathbf{y}}\hat{\mathbf{y}}^T) \sum_{l=0}^{-2} |\langle F_{hl}|F_{el}\rangle_V|^2 f_{hl,el}(\omega) \quad (4)$$

needs to be added. Our choice[6] has been to add it to the bare polarizability. On the other hand the expression of the polarizability in Ref. 5 which was used to derive (4) is definitely a dressed one. As shown above it is all a matter of the electric field with respect to which we define the polarizability. In Ref. 5 the extension of the original Kramers-Heisenberg induction derivation to a corresponding polarizability was at stake. In the original Kramers-Heisenberg paper[23] the choice of the electric field was explicitly the external one. In that derivation the electric field comes out from the matrix element of the perturbation $\hat{H}_D + W$, where W is the part of the perturbation due to the external electric field $\mathbf{E}_X$ (in Ref. 5, $\mathbf{E}_X$) and $\hat{H}_D$ the (dissipative) part due to the internal electric field $\mathbf{E}_I$.[5] In the original Hamiltonian [Eq. (14) of Ref. 5] the perturbation is governed by $\mathbf{A}$ being the unique microscopic vector potential and it is this potential which governs the transition strength's involved. The concept of the polarizability requires a finite integration volume with the atomic volume as its preferred minimum and uses therefore inherently approximate electric fields. In our view the electric field must be external to the quantum mechanics. Therefore we have chosen to define the theoretical quantum mechanical polarizability with respect to the electric field being closest to the microscopic one and that is the applied or average field as defined above. This choice agrees with the approach used in Refs. 13–16. This choice will not change the expression of the polarizability as such, since it affects only the dissipative part $\hat{H}_D$ and that is accounted for already by the Lorentz radiation damping term. For larger systems like a nano-object this does not mean that $\hat{H}_D$ vanishes. There it becomes replaced by the electronic decay mechanisms like electron-electron or electron-phonon interactions, but these are included phenomenologically through the choice of $\gamma(\omega)$, the imaginary part of the complex resonance frequency $\hat{\omega}_{lk}$ between states l and k.[5] Therefore we will use for the bare embedded dynamical polarizability $\alpha_{\mathrm{BE}}(\omega)$ the expression:

$$\alpha_{\mathrm{BE}}(\omega) = \alpha_{\mathrm{BE}} + \Delta\alpha(\omega), \quad (5)$$

where $\Delta\alpha(\omega)$ is the same as used before in Ref. 6 and α_{BE} the bare embedded static polarizability.

B. The hybrid method for embedded dielectric objects

Bare and dressed polarizabilities are generic concepts. To show how they relate to realistic situations and what their specific expressions are, we begin by considering the static polarizability of a spherical body. From this specification we will learn how our hybrid method must be set up. As mentioned already we will leave the case of the ellipsoidal dielectric bodies to the Appendix, but will use the results for the actual calculations.

The classical problem of a dielectric sphere embedded in a different dielectric medium is solved by means of the macroscopic version of the Poisson equation:

$$\nabla \cdot \mathbf{D} = 0,$$

where $\mathbf{D} = \epsilon\epsilon_0\mathbf{E}$ is the dielectric displacement and ϵ the dielectric constant. We introduce the electrostatic potential $\Phi(\mathbf{r})$ in the usual way and because of the cylindrical symmetry of the problem we are left with

$$\frac{1}{r^2}\frac{\partial}{\partial r}\left(r^2\frac{\partial\Phi(\mathbf{r})}{\partial r}\right) + \frac{1}{r^2\sin\theta}\frac{\partial}{\partial\theta}\left(\sin\theta\frac{\partial\Phi(\mathbf{r})}{\partial\theta}\right) = 0. \quad (6)$$

The full details of the derivation can be found in Jackson[17] and we only repeat here what is necessary for the discussion later on. The external field $\mathbf{E}_X(\mathbf{r}) = \mathbf{E}_0 = E_0\hat{\mathbf{z}}$ is brought in through the external potential $\Phi_X(\mathbf{r})$,

$$\Phi_X(\mathbf{r}) = -E_0 r\cos\theta \quad (7)$$

and it is required that the full potential $\Phi(\mathbf{r})$ must equal this potential at infinity. Jackson gives the solution as a series expansion in Legendre polynomials $P_m(\cos\theta)$ for the potentials $\Phi_I(\mathbf{r})$ inside and $\Phi_O(\mathbf{r})$ outside the sphere:

$$\Phi_I(\mathbf{r}) = \sum_{m=0}^{\infty} a_m\left(\frac{r}{R}\right)^m P_m(\cos\theta),$$

$$\Phi_O(\mathbf{r}) = -E_0 r P_1(\cos\theta) + \sum_{m=0}^{\infty} b_m\left(\frac{R}{r}\right)^{m+1} P_m(\cos\theta). \quad (8)$$

This derivation relies entirely upon the macroscopic boundary equations, being that the electrostatic potential must be continuous across the sphere surface and that the normal component of the dielectric displacement must be continuous as well,

$$\Phi_I(\mathbf{r}) = \Phi_O(\mathbf{r}),$$

$$\epsilon\frac{d}{dr}\Phi_I(\mathbf{r}) = \epsilon_m\frac{d}{dr}\Phi_O(\mathbf{r}). \quad (9)$$

In a single action the final shape for the only two nonzero coefficients is obtained,

$$a_1 = -\left(\frac{3\epsilon_m}{\epsilon + 2\epsilon_m}\right)E_0 R,$$

$$b_1 = \left(\frac{\epsilon - \epsilon_m}{\epsilon + 2\epsilon_m}\right)E_0 R. \quad (10)$$

So the final shape for the potentials becomes

$$\Phi_I(\mathbf{r}) = -\left(\frac{3\epsilon_m}{\epsilon + 2\epsilon_m}\right)E_0 r\cos\theta,$$

$$\Phi_O(\mathbf{r}) = -\left[1 - \left(\frac{\epsilon - \epsilon_m}{\epsilon + 2\epsilon_m}\right)\left(\frac{R^3}{r^3}\right)\right]E_0 r\cos\theta. \quad (11)$$

For the construction of the hybrid model the potential is not as useful as the electric fields, which we prefer to write as

$$\mathbf{E}_I(\mathbf{r}) = -\nabla\Phi_I(\mathbf{r}) = \left(\frac{3\epsilon_m}{\epsilon + 2\epsilon_m}\right)\mathbf{E}_0,$$

$$\mathbf{E}_O(\mathbf{r}) = \mathbf{E}_0 + \left(\frac{\epsilon - \epsilon_m}{\epsilon + 2\epsilon_m}\right)R^3\left(\frac{3\hat{\mathbf{r}}\hat{\mathbf{r}}^T - 1}{r^3}\right)\mathbf{E}_0, \tag{12}$$

where we have used the common differentiation rules.

We will rewrite the result for the outer electric field. Therefore we first introduce the excess dipole strength $\mathbf{p}$ by using the continuum induction rule

$$\mathbf{p} = V\Delta\mathbf{P} = \epsilon_0 V(\epsilon - \epsilon_m)\left(\frac{3\epsilon_m}{\epsilon + 2\epsilon_m}\right)\mathbf{E}_0 = 3\epsilon_0 V\epsilon_m\left(\frac{\epsilon - \epsilon_m}{\epsilon + 2\epsilon_m}\right)\mathbf{E}_0, \tag{13}$$

where $\Delta\mathbf{P}$ is the difference between the polarization density inside a sphere with dielectric constant ϵ and one with ϵ_m. $V = \frac{4}{3}\pi R^3$ is the volume of the dielectric sphere. This result yields a definition for the (excess) polarizability α as

$$\alpha = 3\epsilon_0 V\epsilon_m\left(\frac{\epsilon - \epsilon_m}{\epsilon + 2\epsilon_m}\right), \tag{14}$$

where the excess character is clear from the difference between ϵ and ϵ_m in the numerator. When ϵ happens to equal ϵ_m, there is no excess dipole strength. The nano-object is still polarized then, but no more than its surroundings. The outer field (12) can be rewritten now as

$$\mathbf{E}_O(\mathbf{r}) = \mathbf{E}_0 + \frac{1}{\epsilon_m}\overleftrightarrow{\mathbf{t}}(\mathbf{r})\mathbf{p}$$

$$\overleftrightarrow{\mathbf{t}}(\mathbf{r}) = \frac{3\hat{\mathbf{r}}\hat{\mathbf{r}}^T - 1}{4\pi\epsilon_0 r^3}, \tag{15}$$

where $\mathbf{t}(\mathbf{r})$ is the vacuum static transfer kernel from discrete dipole theory.

We can proceed using these rewritten equations to handle systems with more embedded nano-objects. This extension requires no more but the systematic replacement above of the external field $\mathbf{E}_0$ by the local field $\mathbf{E}_L$, as follows:

$$\mathbf{E}_{Li} = \mathbf{E}_0 + \frac{1}{\epsilon_m}\sum_{i\neq j}\overleftrightarrow{\mathbf{t}}_{ij}\mathbf{p}_j, \tag{16}$$

where $\mathbf{t}_{ij}$ is the vacuum intercellular transfer tensor, where the presence of the index ij indicates intercellular character in the notation of this paper. The induction for the excess dipole strength's $\mathbf{p}_i$ becomes

$$\mathbf{p}_i = \overleftrightarrow{\alpha}_i\left(\mathbf{E}_0 + \frac{1}{\epsilon_m}\sum_{i\neq j}\overleftrightarrow{\mathbf{t}}_{ij}\mathbf{p}_j\right), \tag{17}$$

where we return to the dynamic equations by using for $\mathbf{t}_{ij}$ the frequency dependent expressions. We see that although we started our treatment of the embedded dielectric spheres as an exercise in macroscopic dielectric continuum theory, the final result can be directly interpreted as an effectively discrete description. This remark builds the essence of the hybrid method. The system of equations to be solved becomes

$$\overleftrightarrow{\alpha}_i^{-1}\mathbf{p}_i - \frac{1}{\epsilon_m}\sum_{i\neq j}\overleftrightarrow{\mathbf{t}}_{ij}\mathbf{p}_j = \mathbf{E}_0, \tag{18}$$

where α_i is the excess polarizability defined above (14). Here some comment should be given about the influence of the embedding medium upon the polarizability and transfer tensor, commonly called "screening." If we understand screening of a certain quantity as its division by ϵ_m of its unscreened (vacuum) value, then definitely the embedded transfer tensor is screened. This is remarkable, since at first inspection of the result (12) it looks as if there is no screening at all. It is not possible to say whether the polarizability is screened. Again, at first glance it looks as if the ϵ_m in front of the expression for the polarizability (14) is there because of screening. Such interpretation however violates what we have just written about screening. Since the polarizability here is an excess one, there is no properly defined vacuum value to refer to. We return to this point in the next section.

A next question concerns the external field $\mathbf{E}_0$, in the sense of the field applied to the dipole. When the sphere is surrounded by vacuum this field is the external field and it is clear what is meant by that. When the sphere is surrounded by a medium, we have from the result above as an immediate answer that what we have to call here *the external field, is the macroscopic (average) field inside the surrounding medium far from the nano-object*. From this definition it is clear that the excess polarizability (14) is a dressed polarizability.

We determine now the bare and dressed (excess) static polarizabilities for the case of embedded ellipsoidal nano-objects as derived in the Appendix. At forehand we mention already that dressed has nothing to do with screening. Nano-objects either in vacuum or embedded have both dressed and bare polarizabilities, all being different. The dressed embedded polarizability α_{DE} can directly be taken from the Appendix, since the analogy with the dielectric sphere is obvious,

$$\alpha_{\mathrm{DE},u} = \epsilon_0 V\left(\frac{\epsilon_m(\epsilon - \epsilon_m)}{\epsilon_m + N_u(\epsilon - \epsilon_m)}\right)$$

$$N_z = \frac{1}{1-\zeta^2}\left(1 - \frac{\zeta\cos^{-1}\zeta}{\sqrt{1-\zeta^2}}\right) \quad \text{(ellipsoid)},$$

$$N_z = \tfrac{1}{3} \quad \text{(sphere)},$$

$$N_x = N_y = \frac{1 - N_z(\zeta)}{2}, \tag{19}$$

where $u = x, y, z$. We prefer to classify this result as *local electromagnetic*. The bare embedded polarizability α_{BE} follows from a reorganization of the expression for α_{DE}:

$$\alpha_{\mathrm{DE}u} = \frac{\alpha_{\mathrm{BE}}}{1 - t_{Eu}\alpha_{\mathrm{BE}}},$$

$$\alpha_{\mathrm{BE}} = \epsilon_0 V(\epsilon - \epsilon_m), \tag{20}$$

where we see that α_{BE} is an excess quantity too, but it is also not screened. This reorganization yields further the intracellular embedded transfer tensor $\mathbf{t}_E$ which brings in the elec-

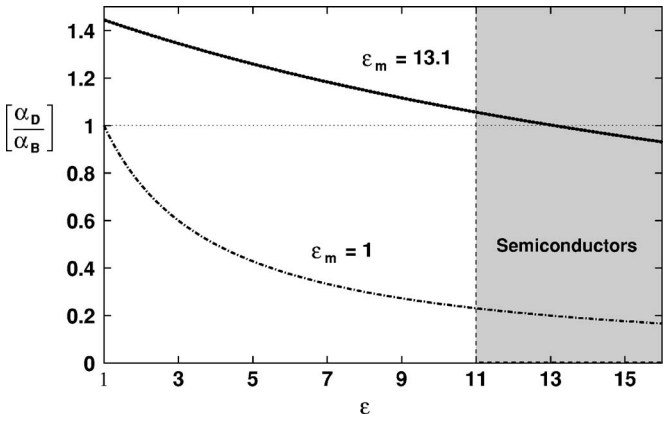

FIG. 2. α_D/α_B for a sphere as a function of its dielectric constant ϵ. Shaded, semiconductor regime.

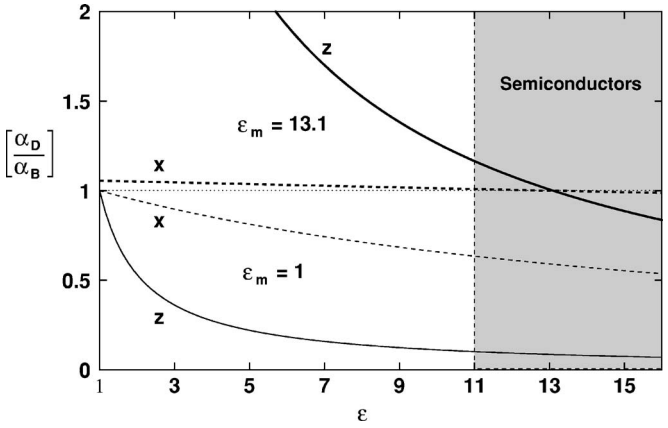

FIG. 3. α_D/α_B for an oblate ellipsoid as a function of its dielectric constant ϵ. Shaded, semiconductor regime. The two upper curves are for $\epsilon_m=13.1$, the embedded case, and the two lower curves are for $\epsilon_m=1$, the vacuum case. x (dashed), z (solid) Cartesian directions.

tromagnetic interactions taking place inside the nano-object, opposite to the intercellular transfer tensors which account for the electromagnetic interactions between nano-objects. Therefore we will classify this result as *nonlocal electromagnetic*. The embedded intracellular transfer tensor $\mathbf{t}_E$ is for ellipsoidal bodies given by

$$t_{Eu} = \frac{1}{\epsilon_m} t_u,$$

$$t_u = -\frac{N_u}{\epsilon_0 V} + \frac{ik^3}{6\pi\epsilon_0}, \tag{21}$$

where $\mathbf{t}$ is the corresponding tensor for the vacuum situation. For embedded nano-objects the intracellular transfer tensor $\mathbf{t}_E$ is screened by ϵ_m, the dielectric constant of the embedding medium. For a nano-object in vacuum the intracellular transfer tensor $\mathbf{t}$ is, in contrast, *not* screened by the dielectric constant ϵ of the nano-object. The dressed polarizability depends on the bare polarizability and on the intracellular transfer tensor. Only that tensor is screened in the case of embedding and only through the influence of that tensor screening enters the dressed embedded polarizability. By itself it is strange that the intracellular transfer tensor happens to be screened by the *surrounding* ϵ_m, but the derivation leaves no other choice. All that can be said to understand it, is that we are dealing with an excess polarizability and not with a full polarizability.

We investigate in detail the behavior of the dressed and bare polarizability. Using the definitions collected in (19) it is easy to give an explicit relation for the ratio between α_D and α_B,

$$\left(\frac{\alpha_D}{\alpha_B}\right) = \frac{\epsilon_m}{\epsilon_m + N_u(\epsilon - \epsilon_m)}. \tag{22}$$

For the case of the dielectric sphere this ratio has been plotted in Fig. 2 as a function of the dielectric function ϵ of the nano-object. For free nano-objects, the vacuum case, the ratio is shown by the dashed line. For semiconductors ϵ is large, above 11, and the bare polarizability is at least 4 times larger than the dressed one. Embedding changes all this. For the case of GaAs we have $\epsilon_m=13.1$ and the dressed to bare ratio is shown by the solid line. Then for embedded semiconductor nano-objects, there is hardly any difference left anymore between the dressed and bare polarizability.

For the oblate ellipsoid-type of nano-objects to be treated further on, the dressed to bare ratio is plotted in Fig. 3. For that case the consequences of embedding upon the ratio are even more outspoken. When we use for the dielectric constant of the nano-object the value $\epsilon=15.15$,[18] the ratio α_D/α_B increases by a factor of 11.9 for the z component and by a factor of 1.8 for the x component. So the increments caused by embedding are highly anisotropic. For values of ϵ below ϵ_m ($\epsilon<13.1$) this results even in a reversal of the anisotropy. For InAs there is not yet reversal, but the anisotropic increment of the dressed polarizability results into an almost disappearance of the externally observable anisotropy. The ratio α_D/α_B is for that case 0.878 for the z direction and 0.991 for the x direction. The consequences are twofold. First the difference between dressed and bare polarizability is almost gone. Next the anisotropy has almost vanished. Both phenomena have the same origin. In the expression for the dressed polarizability the influence of the intracellular transfer tensor $\mathbf{t}$ has been severely weakened by the ϵ_m. Since this tensor is responsible in the nonlocal description for both the dressing and the anisotropy (the bare polarizability is isotropic), it explains both effects.

C. Electromagnetic response

The calculation of the optical response of an embedded square lattice of nano-objects can be performed using the same (Vlieger) expressions[19,20] for the reflected and transmitted electric fields from a square lattice with lattice constant a_L, as used before in Ref. 6 (we leave out transmittance's):

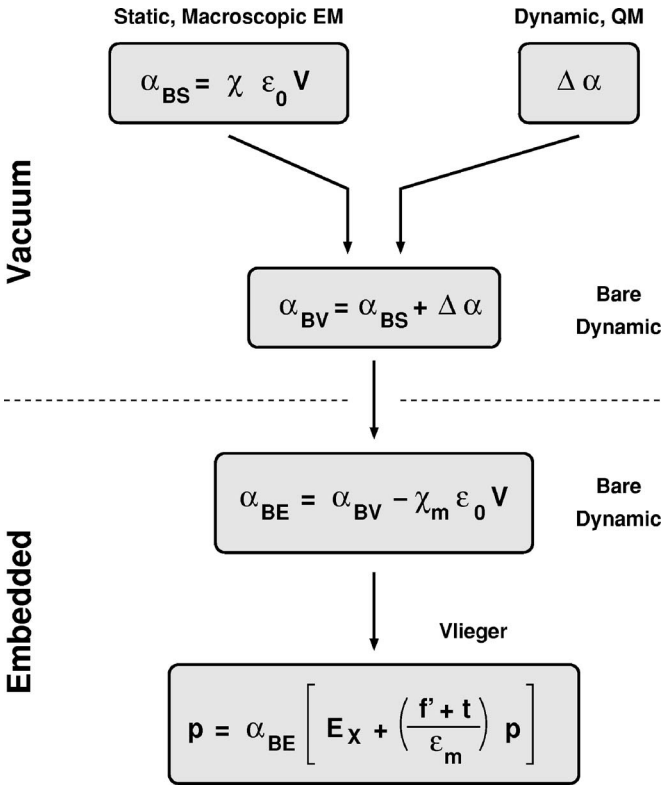

FIG. 4. Flow diagram of process steps to arrive at reflection and transmission for an embedded monolayer of nano-objects. Transfer tensors $\mathbf{f}', \mathbf{t}$ are for vacuum. Susceptibility $\chi = \epsilon - 1$.

$$r_{ss} = \frac{f_k}{A_y \cos\theta_i - f_k},$$

$$r_{pp} = \frac{f_k \cos\theta_i}{A_x - f_k \cos\theta_i} - \frac{f_k \sin^2\theta_i}{A_z \cos\theta_i - f_k \sin^2\theta_i}. \tag{23}$$

The following abbreviations are used to make the expressions more concise, but they contain also all elements which change, when the nano-object gets embedded:

$$A_u = \alpha_0 \alpha_{\mathrm{BE}u}(\omega)^{-1} - \frac{1}{\epsilon_m}(\mathbf{f}'_u + \mathbf{t}_u),$$

$$f_k = 2\pi i a_L k_m, \tag{24}$$

where u is x, y, z and $\alpha_0 = 4\pi\epsilon_0 a_L^3$. We use here the bare excess polarizability (21), since we combine the intracellular transfer tensor $\mathbf{t}$ with the planar transfer tensor $\mathbf{f}$ Refs. 21 and 22 [see also (3)]. Both tensors are made dimensionless through $\mathbf{f} = \alpha_0 f$ and $\mathbf{t} = \alpha_0 t$. All transfer tensors are screened, as described before. An overview of the numerical procedure to determine the dipole strength $\mathbf{p}$ and through that of the optical response is shown in the diagram of Fig. 4. The wave number k_m changes also upon embedding, as will be treated next. Although externally only dressed polarizabilities are observable, the entire theoretical derivation makes only use of bare polarizabilities which definitely improves the transparency of it. Effectively the bare polarizabilities turn into dressed ones through the intracellular transfer tensor $\mathbf{t}$ but this tensor is added only at the last stage, when the Vlieger equations are invoked.

TABLE I. Basic input parameters for lattices of dots. For meaning of symbols see the text and Ref. 6.

	Quantum dot
a_L	80.0 nm
a	18.45 nm
c	1.49 nm
$\lvert\langle F_{h0} \rvert F_{c0}\rangle_V\rvert$	0.9454
$\lvert\langle F_{h,-1} \rvert F_{c,-1}\rangle_V\rvert$	0.9285
$\lvert\langle F_{h,-2} \rvert F_{c,-2}\rangle_V\rvert$	0.9120
r_{ch}	0.60
σ	15.15
σ_m	13.1
E_G (T=0 K)	0.42 eV

Since the Vlieger equations are dynamical they contain the wave number k, which is directly affected by the dielectric constant ϵ_m of the embedding medium, because it follows from the dispersion equation for the embedding medium:

$$\nabla^2 \mathbf{E} - \epsilon_0 \mu_0 \epsilon_m \frac{\partial^2}{\partial t^2} \mathbf{E} = 0.$$

We refer to the wave number inside the medium as k_m and to the vacuum wave number as $k_0 = \omega/c$. The result becomes

$$k_m = \sqrt{\epsilon_m}\frac{\omega}{c} = \sqrt{\epsilon_m} k_0.$$

The embedded wave number k_m turns out to be almost 4 times (3.89) as large as the vacuum wave number k_0 for InAs and affects the reflection coefficients by the same amount, as can be seen from Eq. (23).

III. NUMERICAL RESULTS

We show the results of the influence of embedding upon the optical response of an embedded square lattice of nano-objects for the case of quantum dots. We use the same InAs/GaAs-quantum dots and lattice configuration as studied in Ref. 6 The dots are statically modelled by oblate dielectric ellipsoids with a, c as the long, respectively, short axis. The relevant data are given in Table I. For further details we refer to Ref. 6.

The bare polarizabilities of this system are given as

$$\alpha_{Bx}(\omega) = \alpha_{By}(\omega) = \alpha_B + \Delta\alpha(\omega),$$

$$\alpha_{Bz}(\omega) = \alpha_B, \tag{25}$$

where α_B is as given by the second line of Eq. (20). The addition of the dynamical $\Delta\alpha(\omega)$ restores the anisotropy as we will discuss later. We compare these static bare embedded (excess) polarizabilities α_{BE} to the vacuum bare polarizability α_{BV} of the same quantum dot,

TABLE II. Dressed static polarizability α_D for x,z orientation for vacuum and embedded situation.

	Vacuum	Embedded
α_{Dx}	$2.583\,09\times10^{-3}\ \alpha_0$	$6.731\,66\times10^{-4}\ \alpha_0$
α_{Dz}	$3.467\,74\times10^{-4}\ \alpha_0$	$5.966\,24\times10^{-4}\ \alpha_0$

$$\alpha_{\mathrm{BV}} = 4.672\,45\times10^{-3}\alpha_0,$$

$$\alpha_{\mathrm{BE}} = 6.769\,27\times10^{-4}\alpha_0, \tag{26}$$

where the standard polarizability α_0 has the value 5.69677×10^{-32} Fm^2 for the lattice chosen in Ref. 6. We see that the bare polarizability of this system drops by a factor of 0.145, almost one order of magnitude, as a result of the embedding, because

$$\left(\frac{\alpha_{\mathrm{BE}}}{\alpha_{\mathrm{BV}}}\right) = \left(\frac{\epsilon-\epsilon_m}{\epsilon-1}\right)^D = g_B. \tag{27}$$

The corresponding static dressed polarizabilities depend upon orientation and are given in Table II. The values in the table confirm what we have mentioned before about the general behavior of bare and dressed polarizabilities upon embedding. For the x orientation the embedded polarizability equals 0.26 times the vacuum polarizability, so it drops upon embedding, and for the z orientation it equals 1.72 times the vacuum polarizability, so it increases upon embedding. The anisotropy, the ratio α_x/α_z drops from 7.45 for vacuum to 1.13 for embedded. These anisotropies are the same as the anisotropies in the dressed to bare ratio discussed before. This must be, since the bare polarizability drops out as a common factor in the anisotropy ratio.

The consequences of embedding hence are strong and definitely at first glance counter-intuitive. This holds particularly for the increased dressed polarizability in the z orientation and for the almost disappearance of the anisotropy for such a highly anisotropic body. The reference point to understand this behavior is the bare polarizability, which behaves according to expectation. These bare polarizabilities are isotropic. Only the internal electromagnetic interactions as accounted for by the intracellular transfer tensor, are responsible for the anisotropy of the static dressed polarizabilities. It is the screening of this tensor inside the quantum dot which is responsible for the decreased anisotropy, as argued before. Of course this is a result of choosing excess quantities, but within that choice it is understandable. From Eqs. (22) and (20) it is easy to show that

$$\left(\frac{\alpha_{\mathrm{DE}}}{\alpha_{\mathrm{DV}}}\right)_u = \epsilon_m\left(\frac{1+N_u(\epsilon-1)}{\epsilon_m+N_u(\epsilon-\epsilon_m)}\right)g_B. \tag{28}$$

This expression becomes useful, when we realize that the anisotropy of the ellipsoid is so large that $N_x\approx0$ and $N_z\approx1$. For these two limiting cases we find

$$\left(\frac{\alpha_{\mathrm{DE}}}{\alpha_{\mathrm{DV}}}\right)_x \approx g_B,$$

$$\left(\frac{\alpha_{\mathrm{DE}}}{\alpha_{\mathrm{DV}}}\right)_z \approx \epsilon_m g_B, \tag{29}$$

and the second line shows directly that in the z direction for our quantum dots the dressed embedded (excess) polarizability α_{DE} is larger than its vacuum normal counterpart α_{DV}. Going from vacuum to embedded the bare polarizability decreases. The factor however which turns the bare polarizability into the dressed one [Eq. (22)] increases for the z orientation by an even larger amount. For the x orientation this factor is 1 and has hence no effect. The behavior in the z direction is entirely related to the electromagnetic interactions inside the nano-object and its screening. So both remarkable effects have the same origin: the screening of the intracellular transfer tensor.

The frequency dependent behavior of the x component of the bare polarizability α_B is shown in Fig. 5 and has been calculated using Eqs. (20), (4), and (5). We have used for the damping $\hbar\gamma=5$ meV. The z component of the bare polarizability α_B is constant according to (25) and has the value of α_{BE}, hence

$$\alpha_{Bz} = 6.769\,27\times10^{-4}\alpha_0. \tag{30}$$

In the left-hand panel (a) of Fig. 5 we show the real part of the bare polarizability α_{Bx}. This is the stronger component. For the free floating quantum dots (vacuum embedding) there is just very weak structure in the real part as can be seen in the left-hand panel of Fig. 5. The first strong effect of embedding for the real part is a decrement of the mean value by almost one order of magnitude. The reduction factor is given by $1/g_B$ and the value is 6.9. Simultaneously however the structure due to the quantum mechanical transitions is relatively enhanced. As can be seen from Eq. (21) the responsible mechanism is the subtraction of the embedding dielectric constant ϵ_m. The addition of the dynamic quantum mechanical contribution $\Delta\alpha(\omega)$ to only the x and y component restores the anisotropy, almost lost by the embedding. The picture is quite different for the imaginary part as shown in the right-hand panel (b) of Fig. 5. Since the embedding dielectric constant has no imaginary component in our region of interest, the only imaginary contribution is from $\Delta\alpha(\omega)$. As a result the imaginary part is not influenced by the embedding, as we see in Fig. 5, where the results for vacuum and embedding with $\epsilon_m=13.1$ coincide.

The first (internally) observable optical response term is the reflectance. For a single monolayer these reflectance's are weak. Embedding however does not deteriorate that situation much. For an angle of incidence of $\theta_i=60°$ the reflectance's for the two polarization directions s and p are shown in Fig. 6. This angle is close to the Brewster angle, where s type of reflectance is always (much) stronger than for p type. The left-hand panel (a) shows that there is only weakly decreased

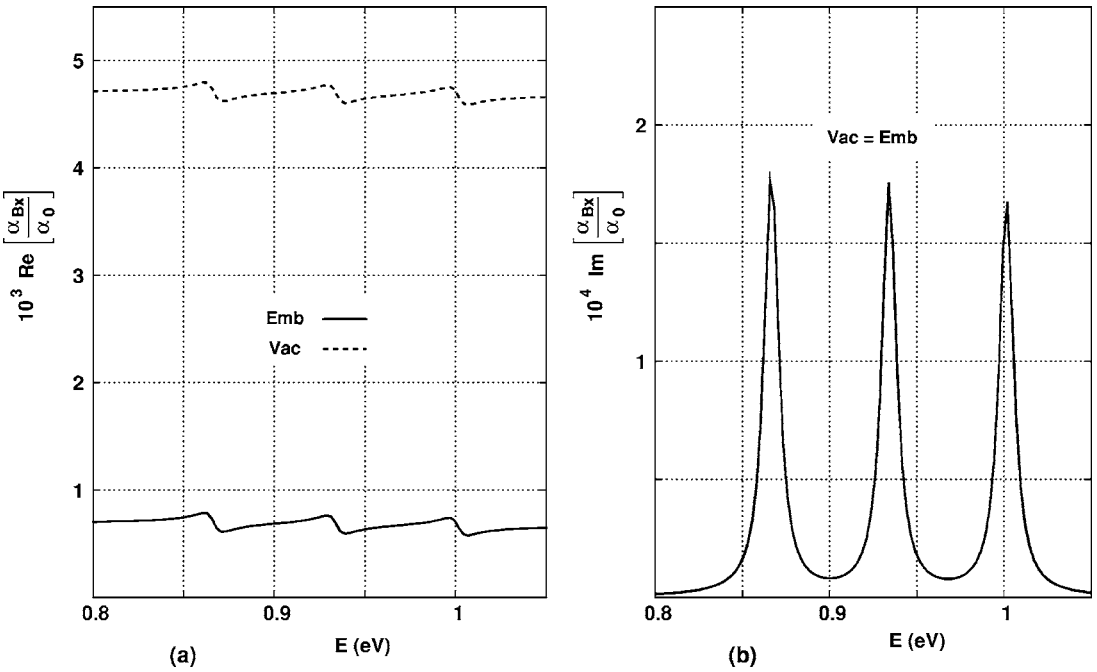

FIG. 5. Bare polarizability α_x. (a) Real part of $\alpha_{B,x}/\alpha_0$, dashed curves, vacuum (no embedding); solid curves, embedding with $\epsilon_m = 13.1$ (b), imaginary part of $\alpha_{B,x}/\alpha_0$ (see text).

reflectance for the *s* component upon embedding. That this is correct can easily be understood. In the denominator of the Vlieger expression for r_{ss}, Eq. (23) the dominant term is $\alpha_0 \alpha_{Bu}^{-1}$. This dominance is so strong that approximately we have that

$$r_{ss} \approx \frac{f_k \alpha_{By}}{\alpha_0 \cos \theta_i}. \tag{31}$$

The bare polarizability α_{By} decreases by the factor g_B being 0.145. This is compensated by the numerator f_k which in-

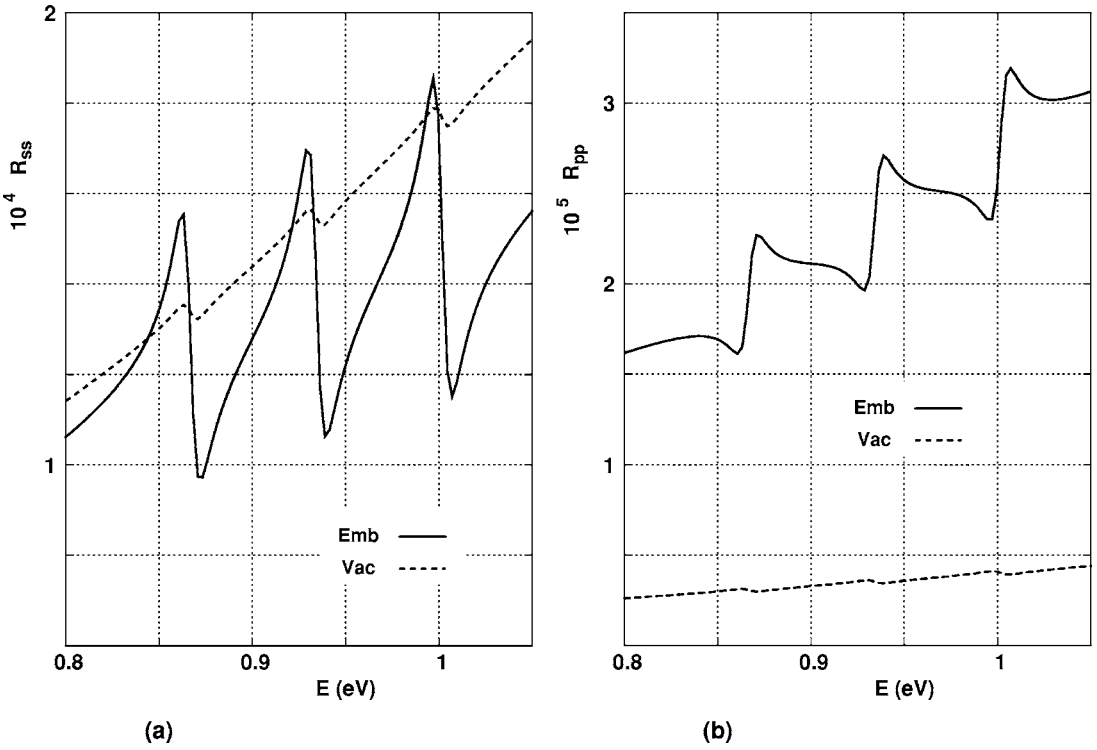

FIG. 6. Reflectance R for angle of incidence $\theta_i = 60°$. (a) R_{ss}, (b) R_{pp}. Dashed curves, vacuum (no embedding); solid curves, embedding with $\epsilon_m = 13.1$.

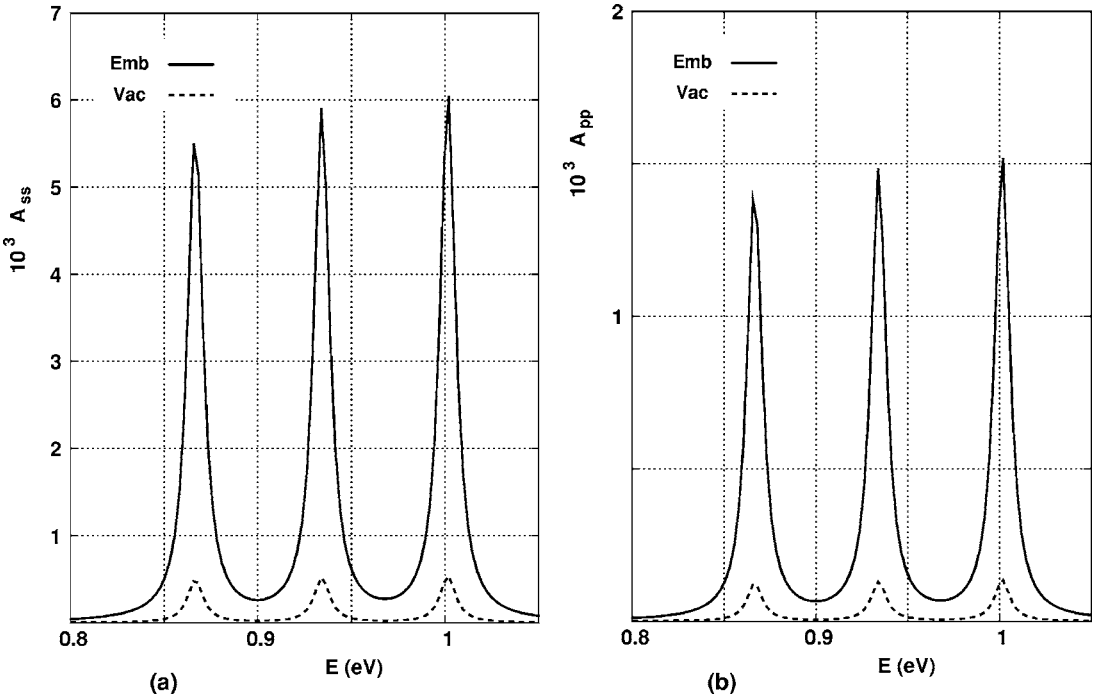

FIG. 7. Absorbance A for angle of incidence $\theta_i=60°$. (a) A_{ss}, (b) A_{pp}. Dashed curves, vacuum (no embedding). Solid curves, embedding with $\epsilon_m=13.1$.

creases with $\sqrt{\epsilon_m}$ or 3.9, but the overall result is a decrement of about 0.6, in agreement with the calculations. For the p component the situation is different. There the embedded reflectance is larger than the vacuum reflectance even up to a factor of 3, but also this is consistent. Roughly the arguments are the same as before for the s component, but now the second term in the expression for r_{pp} becomes the dominant one. Then α_{Bz} takes over and we have mentioned already that this polarizability is larger than its vacuum counterpart. The result is a reflectance larger than for free floating quantum dots. The relevant contribution however is the one due to the quantum mechanical transitions taking place in the quantum dot $\Delta\alpha(\omega)$. This contribution is hardly visible in the vacuum reflectance's, but it gives rise to a strong modulation of the embedded reflectance's. The dynamical structure in the s-component resembles the behavior of the imaginary component of the bare embedded polarizability, whereas the p component resembles its real part.

In Fig. 7 we show the absorbance's for the lattice of quantum dots. At the left, panel (a), are the results for s polarization and at the right, panel (b), for p polarization. The absorbance for p polarization by the free floating dots is about a factor of 4 (peak values) below the absorbance for s polarization. For completely isotropic objects the absorbance for both polarization directions would have been the same. The difference must be ascribed to the anisotropic behavior of the quantum mechanical dynamic part $\Delta\alpha(\omega)$ and has been discussed already in Ref. 6. Both absorbance's, s type and p type have in common that the absorbance for the vacuum case is one order of magnitude below the absorbance for the embedded case. Only because the embedding dielectric constant is not absorbing a simple explanation can be given. We use the continuum description to describe the total power dissipation dU/dt (proportional to the absorbance) inside the dot,

$$\frac{dU}{dt} = \frac{\omega}{2}\epsilon_0 V \epsilon_2 |\langle \mathbf{E} \rangle|^2,$$

$$\langle \mathbf{E} \rangle = \mathbf{E}_I = \left(\frac{\epsilon_m}{\epsilon_m + (\epsilon - \epsilon_m)N_u} \right) E_0 \hat{\mathbf{z}}. \tag{32}$$

Using this result we see that for the electric field in vacuum the external field $\mathbf{E}_X$ (amplitude E_0) hardly can enter the dot. The internal field strength becomes then 0.55 E_0 for the x and 0.074 E_0 for the z direction. Upon embedding the internal field strength becomes 0.99 E_0 for the x and 0.88 E_0 for the z direction. These increased field penetrations are responsible for the increased absorbance. Actually however Fig. 7 shows the excess absorbance, but since the embedding medium is transparent the fast expression above must be assigned completely to the excess.

The ellipsometric angles Ψ and Δ are important because they represent the experimental values which can be measured with the highest accuracy. They obey the definitions

$$\frac{r_{pp}}{r_{ss}} = \tan \Psi e^{i\Delta}. \tag{33}$$

The ellipsometric angles are relative quantities as is clear from the definition in the sense that they do not depend upon the absolute intensities of the reflected light. Yet, since the phase shift Δ, can be obtained separately and independently from the relative intensity variation as represented by Ψ, the full response function can be recovered. In this case this would mean the full polarizability of the embedded dot, if we assume the dielectric constant of the medium to be a known

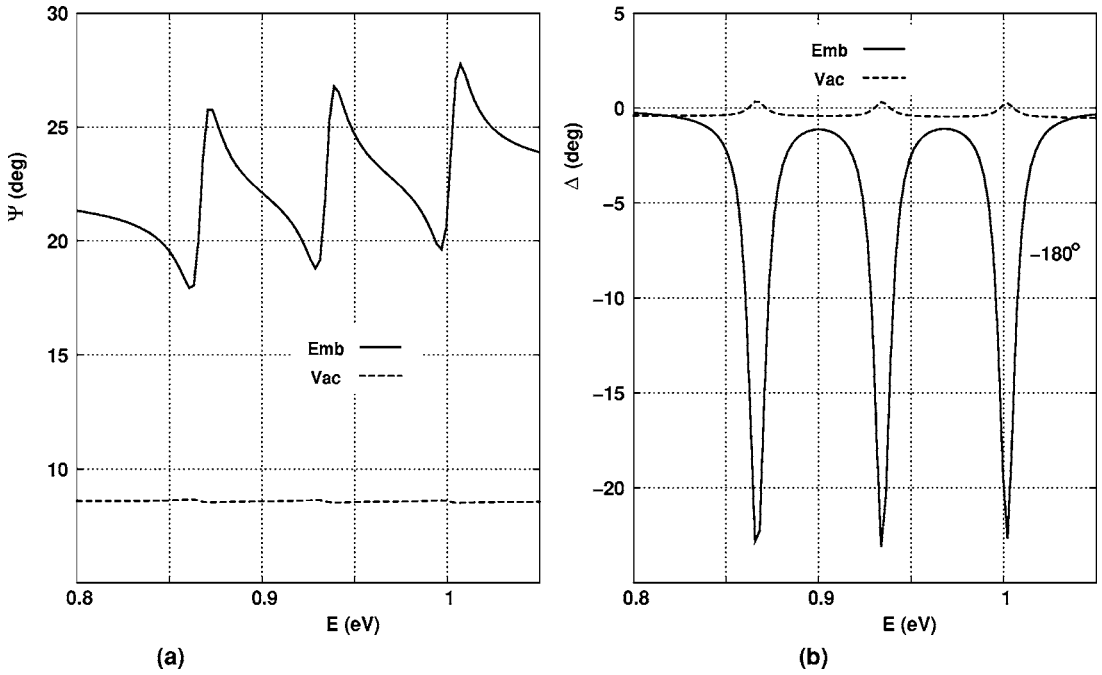

FIG. 8. Ellipsometric angles Ψ, Δ for angle of incidence $\theta_i=60°$. (a) Ψ(°), (b) vacuum, Δ(°); embedded, Δ(°)−180°. Dashed curves, vacuum (no embedding). Solid curves, embedding with $\epsilon_m=13.1$

parameter. For the ellipsometric angle Ψ the vacuum results are systematically below the embedded results, as can be seen in Fig. 8. The value of $\Psi=8.6°$ as an average for the vacuum situation, corresponds to a value of 44 for the ratio between R_{ss} and R_{pp} as found in Fig. 6. The variation of Ψ for the vacuum case is about 2.5% for the investigated region. For the embedded case the situation is very different. The mean value of Ψ centers now around 22.5° in agreement with the fact that the embedded R_{ss} and R_{pp} are one order of magnitude closer to each other now. The absolute variations in Ψ upon embedding have increased by two orders of magnitude as compared to the vacuum case. The observed behavior for Δ cannot be connected to the reflectance's R_{ss} and R_{pp} since in these quantities the phase information is lost. We see that the vacuum and embedded values are 180° out of phase, meaning that r_{ss} and r_{pp} have different sign. Also here the absolute variation in Δ has greatly improved, well over one order of magnitude, upon embedding, but not as large as for Ψ, where the improvement amounts a full two orders of magnitude. The variation in both ellipsometric angles is comfortably within range of an ellipsometer, the weak reflectance, the infrared frequency and the low temperature required for proper measurement conditions being more of a problem.

IV. SUMMARY AND CONCLUSIONS

For a system of nano-objects (here quantum dots) we have derived a hybrid discrete-continuum model to describe the optical response of a square lattice of these dots. It is possible to model the optical behavior of this lattice by means of discrete excess dipoles against a uniform background (including the space occupied by the nano-objects) of the embedding dielectric host medium. For InAs quantum dots with $\epsilon=15.15$ embedded in GaAs with $\epsilon_m=13.1$ and modelled by means of dielectric ellipsoids the excess polarizability of the dot can be larger than the normal polarizability of the same quantum dot in vacuum. All electromagnetic interactions in the system, either between the quantum dots or inside the quantum dot itself, turn out to be screened by the dielectric constant of the host material. This may seem obvious, but the internal electromagnetic interactions inside a free quantum dot are, in contrast, not screened. The dynamical quantum mechanical contributions responsible for both the magnetic field and the frequency dependence are calculated in a Kramers-Heisenberg like fashion and added to the embedded bare polarizability. The first effect of the embedding upon the internal optical response is a decreased reflectance, but no more than a factor of 4. Most other aspects of the response tend to increase upon embedding for the investigated quantum dot host combination. This holds for the structure in the reflectance, the absorbance and particularly for the ellipsometric angles which have increased from measurable (a few tenth of a degree) to large (above 10 degree). Based upon this hybrid model and for this quantum dot host combination the influence of embedding is to increase the effects which can be used for applications.

ACKNOWLEDGMENT

This work is supported by the National Science Council of Taiwan under Contracts Nos. NSC-94-2811-M-009-020 and NSC-94-2112-M-009-037.

APPENDIX: DIELECTRIC OBLATE ELLIPSOID

Although a derivation of the electric fields for an oblate dielectric ellipsoid can be found in Stratton[24] and more recently in Avelin,[25] the expressions given there are not suited for direct use. We will give a straightforward derivation here, using no implicit functions or unresolved integral expressions. Further we will keep the derivation as close as possible to the derivation by Jackson[17] for the spherical case enabling the shortcuts used in this paper. We consider the oblate ellipsoid with short axis c and long axis a as treated in Ref. 6 We will use again $\zeta=c/a$. For the transformation to elliptic coordinates we use

$$x = f \cosh \xi \cos \eta \cos \phi,$$

$$y = f \cosh \xi \cos \eta \sin \phi,$$

$$z = f \sinh \xi \sin \eta, \tag{A1}$$

where $f=\sqrt{a^2-c^2}$. Because of the cylindrical symmetry of the problem (no ϕ dependence) we must solve the following Poisson equation for the electrostatic potential $\Phi(\mathbf{r})$:

$$\left(\frac{\partial^2}{\partial \xi^2} + \tanh \xi \frac{\partial}{\partial \xi} + \frac{\partial^2}{d\eta^2} - \tan \eta \frac{\partial}{\partial \eta}\right)\Phi = 0. \tag{A2}$$

This differential equation can be solved by separation of coordinates,

$$\Phi(\eta, \xi) = G(\eta)F(\xi). \tag{A3}$$

A first solution to this differential equation is the externally applied uniform electric field $\mathbf{E}_0=E_0\hat{\mathbf{z}}$ and its corresponding potential Φ_0:

$$\Phi_0(\eta, \xi, \phi) = -E_0 z = G_0(\eta)F_0(\xi),$$

$$G_0(\eta) = -E_0 f \sin \eta,$$

$$F_0(\xi) = \sinh \xi. \tag{A4}$$

Since the condition $\xi=\xi_0$ establishes the surface of the oblate ellipsoid, varying ϕ, η means scanning this surface. Freezing the η dependence to the one above, reduces the problem to one dimensional.

As a next ingredient to solve the dielectric ellipsoid, we need the solution $F(\xi)$ for a perfectly conducting sphere in a uniform electric field. For this case (A2) becomes

$$\left(\frac{\partial^2}{\partial \xi^2} + \tanh \xi \frac{\partial}{\partial \xi} - 2\right)F(\xi) = 0. \tag{A5}$$

It is readily seen that $F_0(\xi)$ is a solution as is easily verified by substitution. However we need one independent solution more, which can be shown to be

$$F_1(\xi) = 1 - \sinh \xi \tan^{-1}\left(\frac{1}{\sinh \xi}\right). \tag{A6}$$

We will use the functions $F_0(\xi)$ and $F_1(\xi)$ to solve the dielectric case.

The solution for the dielectric ellipsoid is based upon the superposition

$$\Phi_v(\xi, \eta, \phi) = G_0(\eta)[A_v F_0(\xi) + B_v F_1(\xi)], \tag{A7}$$

where the index v equals I for the inner and O for the outer region of the ellipsoid, making four unknowns in total. Two of the unknowns can be eliminated by requiring that the electric field inside is constant and that the electric field outside for large ξ must coincide with the externally applied field $\mathbf{E}_0$. As a result $B_I=0$ and $A_O=1$. The remaining coefficients A_I, B_O follow from the boundary conditions:

$$\Phi_I(\xi_0) = \Phi_O(\xi_0),$$

$$\epsilon \left.\frac{d\Phi_I(\xi)}{d\xi}\right|_{\xi=\xi_0} = \epsilon_m \left.\frac{d\Phi_O(\xi)}{d\xi}\right|_{\xi=\xi_0} \tag{A8}$$

which yields as a system of equations

$$\begin{Vmatrix} 1 & -h_1 \\ \epsilon & -\epsilon_m h_2 \end{Vmatrix} \begin{vmatrix} A_I \\ B_O \end{vmatrix} = \begin{vmatrix} 1 \\ \epsilon_m \end{vmatrix},$$

where the factors h_1, h_2 are given by

$$h_1 = \frac{F_1(\xi_0)}{F_0(\xi_0)} = \frac{1}{\sinh \xi_0} - \tan^{-1}\left(\frac{1}{\sinh \xi_0}\right),$$

$$h_2 = \frac{F_1'(\xi_0)}{F_0'(\xi_0)} = \frac{\sinh \xi_0}{\cosh^2 \xi_0} - \tan^{-1}\left(\frac{1}{\sinh \xi_0}\right), \tag{A9}$$

and we find the coefficients A_I and B_O to be

$$A_I = \frac{\epsilon_m(h_1 - h_2)}{\epsilon h_1 - \epsilon_m h_2},$$

$$B_O = \frac{\epsilon_m - \epsilon}{\epsilon h_1 - \epsilon_m h_2}. \tag{A10}$$

We use A_I to determine the electric field inside the ellipsoid,

$$E_I = A_I E_0 = \frac{\epsilon_m(h_1 - h_2)}{\epsilon_m(h_1 - h_2) + (\epsilon - \epsilon_m)h_1} E_o \tag{A11}$$

with which we can determine the polarizability α and the excess polarizability α_X used in this paper (as α),

$$\alpha \mathbf{E}_0 = V\mathbf{P} = \epsilon_0 V \chi E_I = \epsilon_0 V \epsilon_m \left(\frac{\epsilon - 1}{\epsilon_m + (\epsilon - \epsilon_m)N_z}\right)\mathbf{E}_0,$$

$$\alpha_X \mathbf{E}_0 = V(\mathbf{P} - \mathbf{P}_m) = \epsilon_0 V(\chi - \chi_m)E_I$$

$$= \epsilon_0 V \left(\frac{\epsilon_m(\epsilon - \epsilon_m)}{\epsilon_m + N_z(\epsilon - \epsilon_m)}\right)\mathbf{E}_0,$$

$$N_z = \frac{h_1}{h_1 - h_2}, \tag{A12}$$

where $V=\frac{4}{3}\pi a^2 c$ is the volume of the ellipsoid and the susceptibility $\chi=\epsilon-1$. The depolarization factor N_z is exclusively determined by the values of the eigenfunctions of the problem at the boundary ξ_0 and accounts for the shape dependence. To make the expression more accessible we use that

$$\sinh \xi_0 = \frac{c}{\sqrt{a^2 - c^2}} = \frac{\zeta}{\sqrt{1 - \zeta^2}} \tag{A13}$$

and this enables us to write

$$h_1 = \frac{\sqrt{1-\zeta^2}}{\zeta} - \tan^{-1}\left(\frac{\sqrt{1-\zeta^2}}{\zeta}\right),$$

$$h_1 - h_2 = \frac{(1-\zeta^2)^{3/2}}{\zeta}, \tag{A14}$$

and we find for the depolarization factor N_z,

$$N_z = \frac{1}{1-\zeta^2}\left(1 - \frac{\zeta \cos^{-1}\zeta}{\sqrt{1-\zeta^2}}\right) \tag{A15}$$

which is exactly the same as the depolarization factor obtained by Avelin[25] and for $\epsilon_m = 1$ this depolarization factor produces also Avelin's polarizability when used in (A12). For the treatment of the embedded case when $\epsilon_m > 1$ the reader is referred to the text.

The real benefit of this derivation is in the expressions for the external field $\mathbf{E}_O(\mathbf{r})$,

$$\mathbf{E}_O(\mathbf{r}) = \mathbf{E}_0 - B_O \nabla G_0(\eta) F_1(\xi) = \mathbf{E}_0 + \mathbf{E}_E(\mathbf{r}). \tag{A16}$$

We refrain from the details and give only the final result in cylindrical coordinates,

$$\mathbf{E}_E(\mathbf{r}) = E_\rho \hat{\boldsymbol{\rho}} + E_z \hat{\mathbf{z}},$$

$$\mathbf{r} = \rho\hat{\boldsymbol{\rho}} + z\hat{\mathbf{z}} = \sqrt{x^2 + y^2}\hat{\boldsymbol{\rho}} + z\hat{\mathbf{z}},$$

$$\hat{\boldsymbol{\rho}} = \cos\phi\hat{\mathbf{x}} + \sin\phi\hat{\mathbf{y}}, \tag{A17}$$

where the component fields E_ρ, E_z are given by

$$E_\rho = -E_0 B_O\left(\frac{\tilde{z}\tilde{\rho}\sqrt{S}}{(S^2 + \tilde{z}^2)(1+S)}\right),$$

$$E_z = -E_0 B_O\left[\tan^{-1}\left(\frac{1}{\sqrt{S}}\right) - \frac{S\sqrt{S}}{S^2 + \tilde{z}^2}\right],$$

$$B_O = -\frac{\zeta}{(1-\zeta^2)^{3/2}}\left(\frac{(\epsilon - \epsilon_m)}{\epsilon_m + (\epsilon - \epsilon_m)N_z(\zeta)}\right), \tag{A18}$$

where the crucial auxiliary variable S is defined by

$$S = \sqrt{s^2 + \tilde{z}^2} - s,$$

$$s = \tfrac{1}{2}[1 - (\tilde{\rho}^2 + \tilde{z}^2)], \tag{A19}$$

where $\tilde{u} = u/f$ $u = \rho, z$. Using these expressions for the outer field, backtransformation to cylindrical coordinates is established, but those coordinates are equivalent to Cartesian, because of the cylindrical symmetry of the problem. Since the outer electric field expressions are explicit functions of the Cartesian coordinates, they are suited for direct use.

[1] V. G. Veselago, Sov. Phys. Usp. **10**, 509 (1968).
[2] J. B. Pendry *et al.*, IEEE Trans. Microwave Theory Tech. **47**, 2075 (1999).
[3] O. Voskoboynikov, G. Dyankov, and C. M. J. Wijers, Microelectron. J. **36**, 564 (2005).
[4] R. A. Shelby, D. R. Smith, and S. Schulz, Science **292**, 79 (2001).
[5] C. M. J. Wijers, Phys. Rev. A **70**, 063807 (2004).
[6] O. Voskoboynikov, C. M. J. Wijers, J. L. Liu, and C. P. Lee, Phys. Rev. B **71**, 245332 (2005).
[7] C. M. J. Wijers and P. L. de Boeij, J. Chem. Phys. **116**, 328 (2002).
[8] O. Stier, M. Grundmann, and D. Bimberg, Phys. Rev. B **59**, 5688 (1999).
[9] G. W. Bryant, Phys. Rev. B **37**, 8763 (1988).
[10] P. Enders, A. Bärwolff, M. Woerner, and D. Suisky, Phys. Rev. B **51**, 16695 (1995).
[11] J. I. Climente, J. Planelles, and W. Jaskolski, Phys. Rev. B **68**, 075307 (2003); J. Climente *et al.*, J. Phys.: Condens. Matter **15**, 3593 (2003).
[12] C. G. Darwin, Proc. R. Soc. London, Ser. A **146**, 17 (1934).
[13] P. Noziéres and D. Pines, Phys. Rev. **109**, 762 (1958).
[14] O. Keller, J. Opt. Soc. Am. B **11**, 1480 (1994).
[15] S. L. Adler, Phys. Rev. **126**, 413 (1962).
[16] N. Wiser, Phys. Rev. **129**, 62 (1963).
[17] J. D. Jackson, *Classical Electrodynamics* (Wiley, New York, 1972).
[18] S. L. Chuang, *Physics of Optoelectronic Devices* (Wiley, New York, 1995).
[19] J. Vlieger, Physica (Amsterdam) **64**, 63 (1973); C. M. J. Wijers and K. M. E. Emmett, Phys. Scr. **38**, 435 (1988).
[20] O. Litzman and P. Rózsa, Surf. Sci. **66**, 542 (1977).
[21] G. P. M. Poppe, C. M. J. Wijers, and A. van Silfhout, Phys. Rev. B **44**, 7917 (1991).
[22] C. M. J. Wijers and G. P. M. Poppe, Phys. Rev. B **46**, 7605 (1992).
[23] H. A. Kramers and W. Heisenberg, Z. Phys. **31**, 681 (1925).
[24] J. A. Stratton, *Electromagnetic Theory* (McGraw-Hill, New York, 1941).
[25] J. Avelin, Ph.D. thesis, Electromagnetics Laboratory, Helsinki University of Technology, Report 414, 2003.